Int. J. Electrochem. Sci., 13 **(2018)** 10259 – 10273, doi: 10.20964/2018.11.69

International Journal of
ELECTROCHEMICAL
SCIENCE
www.electrochemsci.org

Electrochemical Detection of Trace Cadmium and Lead on a MCM41/Nafion/Antimony Film Composite-Modified Electrode

Yuan Yin[1,2], *Hui Wang*[1,2], *Gang Liu*[1,2,*]

[1] Key Lab of Modern Precision Agriculture System Integration Research, Ministry of Education of China, China Agricultural University, Beijing 100083 P. R. China
[2] Key Lab of Agricultural Information Acquisition Technology, Ministry of Agricultural of China, China Agricultural University, Beijing 100083 P. R. China
[*]E-mail: pac@cau.edu.cn

Received: 10 November 2017 / *Accepted:* 25 December 2017 / *Published:* 1 October 2018

In the current work, an MCM41, Nafion and stibonium (Sb) composite-modified electrode was prepared to analyze trace cadmium (Cd) and lead (Pb) concentrations via square wave anodic stripping voltammetry (SWASV). The morphology and electrochemical properties of the modified electrode were characterized through cyclic voltammetry (CV) and electrochemical impedance spectroscopy (EIS). The results suggested that the MCM41 layer that formed on the glassy carbon electrode (GCE) enhanced the adsorption capacity for Cd(II) and Pb(II) and increased the specific surface area of the electrode. In addition, the Nafion film effectively improved the adhesion and stability of the MCM41 layer. The synergistic effect in the Sb film for Cd(II) and Pb(II) increased the stripping current. The obtained electrode exhibited an effective stripping property for analyzing Cd(II) and Pb(II). Importantly, a linear response was obtained within the range 5-30 $\mu g \cdot L^{-1}$ under optimal conditions, and the limits of detection (LOD) for Cd(II) and PB(II) were 0.29 $\mu g \cdot L^{-1}$ and 0.08 $\mu g \cdot L^{-1}$, respectively.

Keywords: MCM41, Nafion, Antimony film, Electrochemical detection, Modified electrode

1. INTRODUCTION

Heavy metals are a major source of environmental pollution, and they exert marked negative effects on ecological quality. Cadmium (Cd) and lead (Pb) are toxic heavy metals that can significantly affect human health. Heavy metals frequently accumulate in the environment due to their long-term chemical stability and non-degradability [1-3]. Heavy metals in soil can be absorbed by plants and decrease plant growth. These soil pollutants can enter the bodies of domestic animals or humans via the food chain, leading to immediate or long-term health risks. The demand for heavy metal detection

has increased over the past few years, and a rapid analytical method to detect heavy metals is required [4-6].

An electrochemical stripping analysis (ESA) has advantages such as a remarkable sensitivity, rapid analysis, good selectivity and low cost, and ESA is an effective method to measure trace heavy metal concentrations. Traditionally, a mercury (Hg) electrode has been used in ESA measurements. However, the high toxicity of Hg and the risks involved in its management are unfavorable. Similar to the bismuth (Bi) film-modified electrode, the stibonium (Sb) film-modified electrode has been introduced as a substitute for the Hg electrode due to its advantages, such as a low toxicity, high sensitivity and large cathode potential range [7-8]. Additionally, glassy carbon electrodes (GCEs) have become the most commonly used electrodes in electrochemical analyses due to their non-toxicity, strong electrical conductivity, high cathode potential range and reusability [9].

Sample analyses have indicated that surface-active materials can adsorb onto electrode surfaces and inactivate the electrode. An effective method to reduce the adsorption layer is coating the electrode with a dialysis film such as Nafion [10]. However, a solvent evaporation process is involved in the modification process, resulting in poor homogeneity and reproducibility of the films. Composite modification is an effective method that possesses advantages such as a high stability, strong adhesive force, and controllable structure and film thickness [11-12]. MCM41 is a highly ordered, arranged, silicon-based, mesoporous material with a high porosity, favorable electrical properties, good chemical stability and a large specific surface area [13-15]. These properties have resulted in broad application prospects for MCM41 in electrochemical sensor research [16].

In the current study, a composite-modified electrode was prepared using an MCM41 dispersion and a Nafion solution and was followed by drying under light. At the beginning of the experiment, an Sb standard solution was slowly added into the buffer solution. Trace Cd and Pb ion concentrations were detected on the prepared electrodes using square wave anodic stripping voltammetry (SWASV). The results suggested that the MCM41/Nafion/Sb film composite-modified electrode had a higher sensitivity than the Nafion-modified bare GCEs. This was because the Nafion-modified MCM41 electrode had a favorable mechanical stability, large active surface area, superb conductivity, effective ion exchange, strong capacity to resist disturbances, low Sb film toxicity, high sensitivity and large cathode potential range.

2. EXPERIMENTAL

2.1 Instruments and Reagents

The electrochemical measurements were conducted using the CHI660D electrochemical workstation (Shanghai CH Instruments, China). A three-electrode system was adopted with a modified GCE working electrode (Φ = 3 mm), Ag/AgCl reference electrode and platinum electrode. All electrochemical measurements were carried out in a 25 mL cell.

MCM41 was purchased from XFNANO Materials Tech Co., Ltd. (Nanjing, China). The Nafion solution was obtained from DuPont Co., Ltd. and diluted to a concentration of 0.5%. Ethyl alcohol, aluminum oxide powder and nitrate of potash were obtained from Macklin Biochemical Co., Ltd. (Shanghai, China). Potassium ferricyanide and potassium ferrocyanide were purchased from Jinke

Institute of Fine Chemical Engineering (Tianjin). The Cd(II), Pb(II), Bi(III) (1000 $mg \cdot L^{-1}$) and Sb(III) (1000 $mg \cdot L^{-1}$) stock solutions were obtained from the China State Center for Standard Matter and diluted as required. The acetate buffer was purchased from Obiolab Co., Ltd. (Beijing, China) and used as the supporting electrolyte to detect Cd(II) and Pb(II). Ultrapure water (18.2 $M\Omega \cdot cm^{-1}$) was used for all experiments.

2.2 Preparation of MCM41, Nafion and GCE

Prior to modification, the GCE was polished using 5 μm aluminum oxide powder, rinsed with ultrapure water, and ultrasonically cleaned for 5 min in ultrapure water and straight alcohol. The MCM41 was weighed (4 mg) and added to 1 mL of ultrapure water. Then, MCM41 was ultrasonically dispersed in ultrapure water for 30 min to form a 4 $mg \cdot mL^{-1}$ MCM41 suspension. Subsequently, 5 μL of the suspension was dropped onto the GCE surface after 10 min of stirring, and the modified GCE was dried using a drying light for 2 min and air drying. Afterwards, 2 μL of a 1% Nafion solution was dropped onto the GCE surface, and the modified electrode was dried in the air to obtain the MCM41/Nafion-modified electrode. The other electrodes were also prepared as a comparison using the same method.

2.3 Electrochemical Measurements

The initial exploration of Cd(II) and Pb(II) by SWASV was conducted in a 0.1 M acetate buffer solution (pH 4.5) in the presence of 500 $\mu g \cdot L^{-1}$ Bi(III) and 500 $\mu g \cdot L^{-1}$ Sb(III). Under stirring, a deposition potential of -1.4 V was applied to the working electrode for 120 s. After a standing time of 10 s, a SWASV potential scan was conducted from -1.4 to 0.2 V (square wave amplitude, 25 mV; potential step, 5 mV; frequency, 25 Hz). Before the next cycle, a 120 s cleaning step at 0.3 V with stirring was performed to remove residual cadmium and lead ions.

3. RESULTS AND DISCUSSION

3.1 Basic Characteristics of the Modified Electrodes

Fig. 1 compares the cyclic voltammetry (CV) responses of the GCE, Nafion/GCE and MCM41/Nafion/GCE in 5 mM $[Fe(CN)_6]^{3-/4-}$ solutions. A pair of definite redox peaks were observed on the bare GCE, and they were ascribed to the reversible single electron redox behavior of ferricyanide. After the GCE modification, a pair of markedly reduced redox peaks was observed in the CV curves of Nafion/GCE and MCM41/Nafion/GCE. This indicated that Nafion acted as a cation exchange film to block electron exchange and a barrier layer to decrease interface charge transfer [17-18]. According to Fig. 2, the redox peak current remarkably increased on MCM41/Nafion/GCE compared with that on Nafion/GCE, and this increase could be due to the presence of MCM41, which has a high porosity and large specific surface area and can provide sites to accelerate charge transfer.

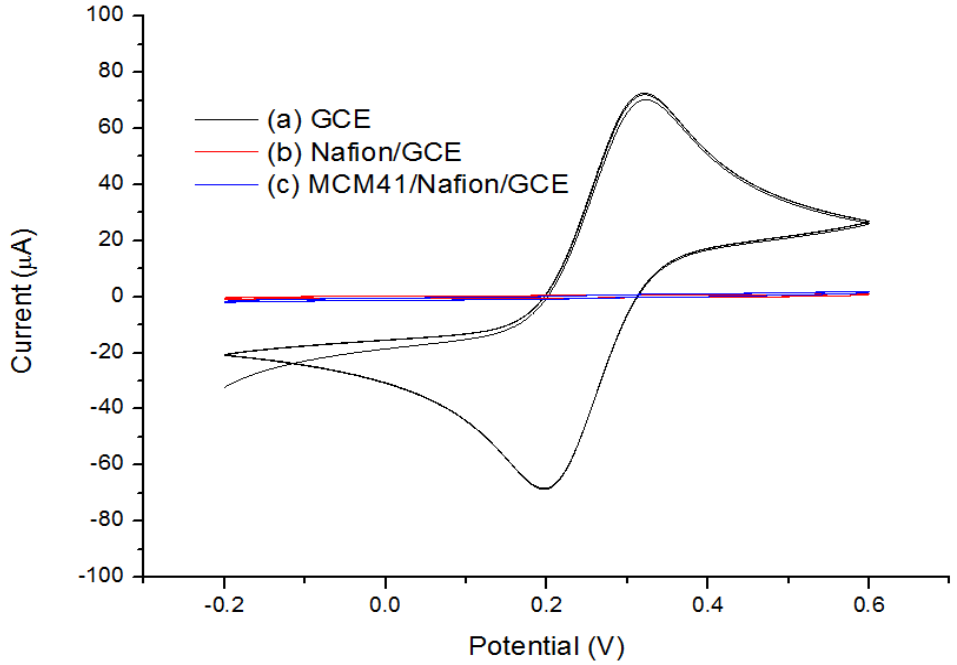

Figure 1. CV curves of 5 mM $[Fe(CN)_6]^{3-/4-}$ in 0.1 M KCl on (a) GCE, (b) Nafion/GCE and (c) MCM41/Nafion/GCE. Scan rate: 50 $mV \cdot s^{-1}$. Initial potential: -0.2 V. Low potential: -0.2 V. High potential: 0.6 V.

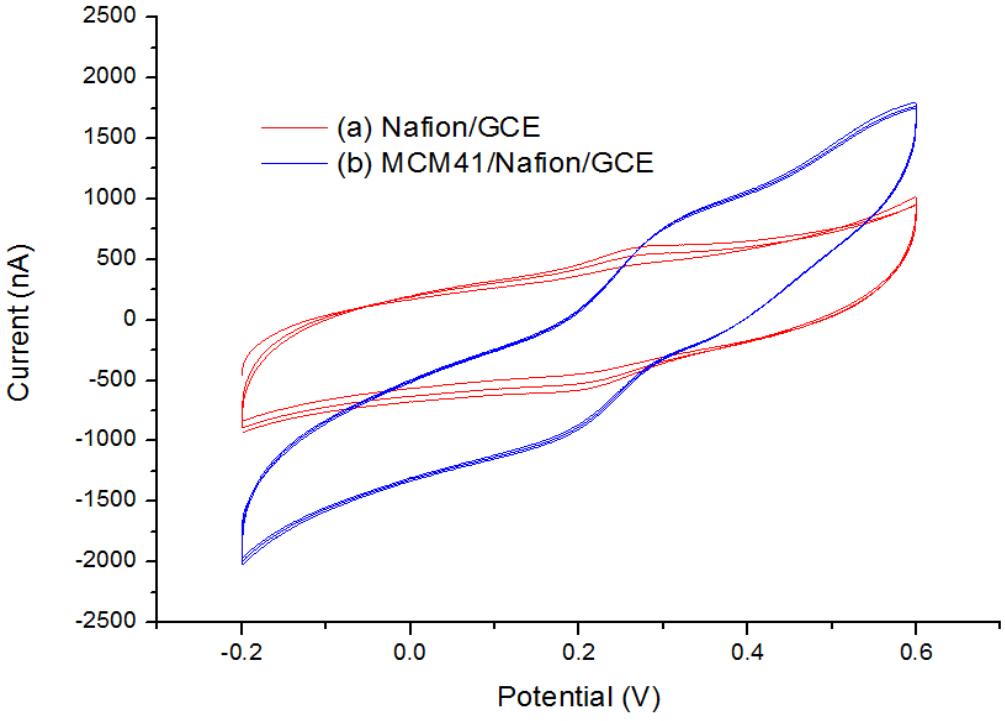

Figure 2. CV curves of 5 mM $[Fe(CN)_6]^{3-/4-}$ in 0.1 M KCl on (a) Nafion/GCE and (b) MCM41/Nafion/GCE. Scan rate: 50 $mV \cdot s^{-1}$. Initial potential: -0.2 V. Low potential: -0.2 V. High potential: 0.6 V.

The electron transfer dynamics of the prepared electrodes were further measured using electrochemical impedance spectroscopy (EIS). Based on Fig. 3, the bare GCE exhibited an extremely

low impedance, while Nafion/GCE had a higher impedance, which suggested that the Nafion blocked the interface electron transfer [19-20]. In addition, a decreased impedance was observed on the MCM41/Nafion/GCE. Enhanced electron transfer dynamics have also been observed for other MCM41-modified electrodes, indicating that MCM41 can enhance the electron transfer rate of an electrode by acting as an electron transfer channel [21].

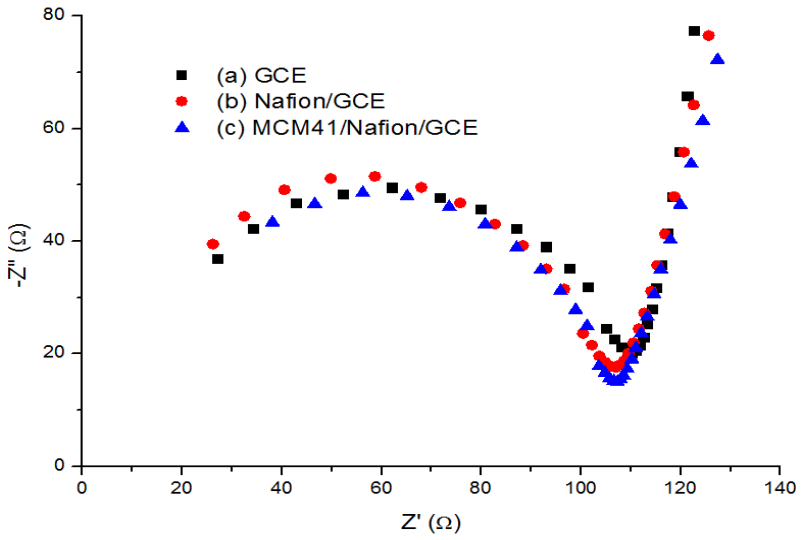

Figure 3. Nyquist plots of 5 mM $[Fe(CN)_6]^{3-/4-}$ on (a) GCE, (b) Nafion/GCE and (c) MCM41/Nafion/GCE in 0.1 M KCl. Initial potential: 0.358 V. High frequency: 1.6×10^6 Hz. Low frequency: 1 Hz. Amplitude: 0.005 V.

3.2 Stripping Response of the Prepared Electrodes

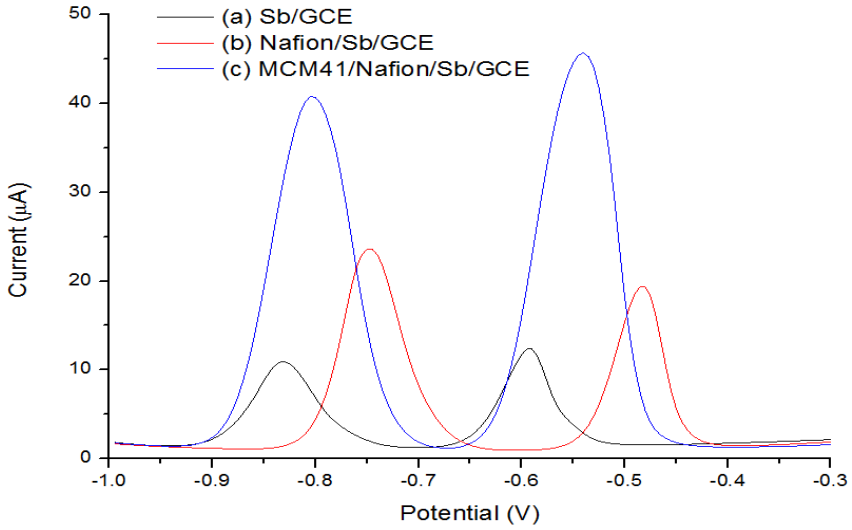

Figure 4. SWASV responses of 20 $\mu g \cdot L^{-1}$ Cd(II) and Pb(II) in a 0.1 M acetate buffer solution (pH 3.5): (a) Sb/GCE, (b) Nafion/Sb/GCE, and (c) MCM41/Nafion/Sb/GCE. Deposition time: 400 s. Deposition potential: -1.0 V. Sb(III) concentration: 2000 $\mu g \cdot L^{-1}$.

Fig. 4 shows the SWASV responses of 20 μg·L^{-1} Cd(II) and Pb(II) on different working electrodes. Obviously, Cd(II) and Pb(II) had poor responses on Sb/GCE (20 μL of a Sb standard solution, 1000 μg/ mL) in the buffer and only displayed two weak peaks. This could be because the added Sb formed an alloy with Cd and Pb on the electrode surface, which accelerated the deposition and dissolution of Cd(II) and Pb(II) on the electrode surface [22]. In addition, the Nafion/Sb/GCE peak current was enhanced by adding 2 μL of a Nafion solution (1%) onto the GCE, and this can be attributed to the hydrophilic sulfonic acid groups on the Nafion film, which contribute to the adsorption of cations (such as Cd, Pb and zinc (Zn)) by other inorganic substances. Therefore, Nafion possesses a positive cation exchange effect [23]. A higher stripping current was observed on MCM41/Nafion/Sb/GCE than on Nafion/Sb/GCE, which can be ascribed to the large specific surface area and special 1-dimensional mesoporous structure of MCM41 providing a large number of adsorption sites for Cd(II) and Pb(II).

3.3. Optimization of the Experimental Conditions

To optimize the performance of the prepared electrodes, the 20 μg·L^{-1} Cd(II) and Pb(II) SWASV responses were employed to study the different experimental parameters in a 0.1 mM acetate buffer.

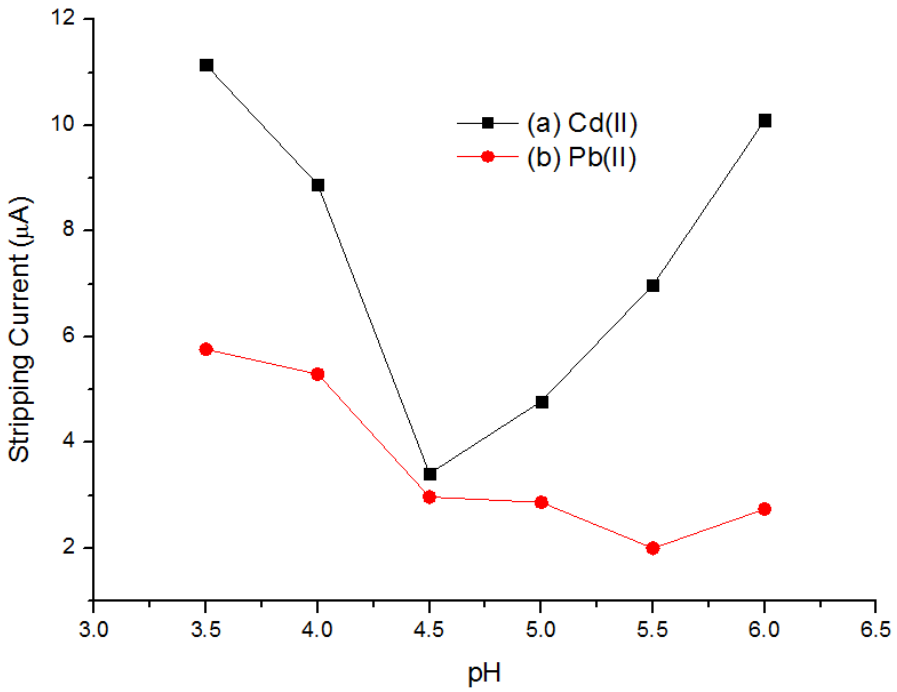

Figure 5. Relationship between the pH of the acetate buffer solution and the stripping currents of (a) Cd(II) and (b) Pb(II). Cd(II) and Pb(II) concentrations: 20 μg·L^{-1}. Deposition time: 120 s. Deposition potential: -1.4 V. Bi(III) concentration: 500 μg·L^{-1}. Sb(III) concentration: 500 μg·L^{-1}.

The dissolution reactions of Cd(II) and Pb(II) were closely related to the pH value of the

acetate buffer solution. Fig. 5 shows the relationship between the pH value of the acetate buffer solution and the stripping currents of Cd(II) and Pb(II). The largest Cd(II) and Pb(II) stripping currents were observed at a pH of 3.5. Meanwhile, the smallest Cd(II) stripping current was observed at a pH of 4.5, and the Cd(II) stripping current increased as the pH increased. In contrast, the Pb(II) stripping current decreased as the pH increased, and the current only slightly increased at a pH of 6.0. These observations can be attributed to two factors. First, the resultant Sb film can improve the electron transfer rate of the electrode at low pH values. The film could be easily hydrolyzed as the pH increases, which could reduce the alloy deposition on the electrode surface and the dissolution current [24]. Second, as the pH increases, Sb and bismuth (Bi) form an alloy with a complicated structure, which could increase the stripping current [25]. Therefore, an acetate buffer solution with a pH of 3.5 was selected as the optimum medium for further experiments. Fig. 6 shows the effect of the deposition potential on the Cd(II) and Pb(II) stripping responses. The largest Cd(II) and Pb(II) peak currents occurred at approximately -0.9 V, and this might be because the excessively low deposition potential promoted the hydrogen evolution reaction and reduced the stripping peak current. Meanwhile, the Cd(II) and Pb(II) stripping currents increased within the deposition potential range of -1.7 V to -0.9 V. The largest stripping currents occurred at approximately -0.9 V, but the Cd(II) stripping current was not completely displayed, as shown in Fig. 7. Therefore, the optimal deposition potential was -1.0 V.

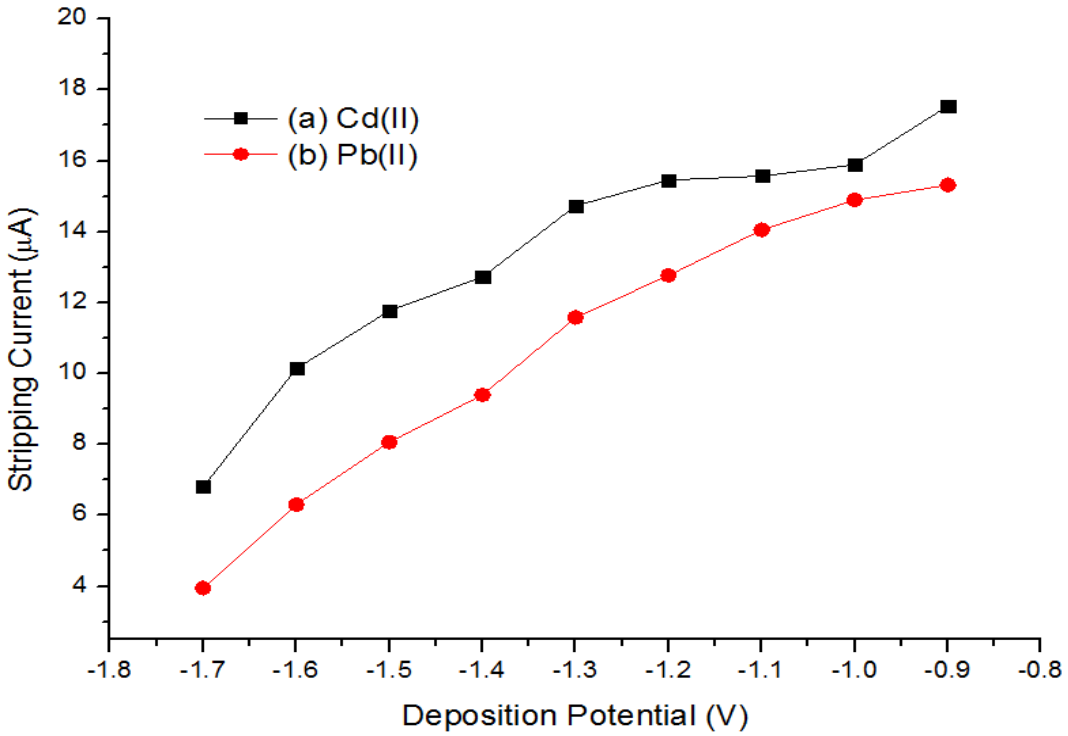

Figure 6. Relationship between the deposition potential and the Cd(II) and Pb(II) stripping peak currents. Cd(II) and Pb(II) concentrations: 20 μg·L^{-1}. Deposition time: 120 s. pH: 3.5. Bi(III) concentration: 500 μg·L^{-1}. Sb(III) concentration: 500 μg·L^{-1}.

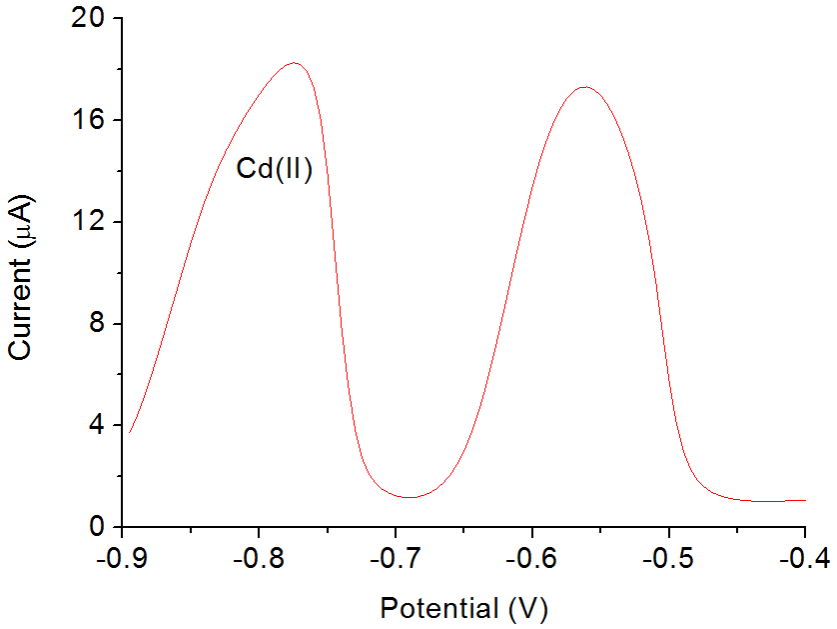

Figure 7. Incomplete stripping current waveform of Cd(II). Cd(II) and Pb(II) concentrations: 20 μg·L^{-1}. Deposition time: 120 s. pH: 3.5. Deposition potential: -0.9 V. Bi(III) concentration: 500 μg·L^{-1}. Sb(III) concentration: 500 μg·L^{-1}.

Fig. 8 shows the effect of the deposition time (within 60-600 s) on the Cd(II) and Pb(II) stripping responses. The largest Cd(II) and Pb(II) current peaks occurred at a deposition time of 600 s, which might be due to metal-ion enrichment on the prepared electrode surface as the deposition time increased. However, the metal-ion enrichment on the electrode surface reached a saturation point after a long deposition time. Therefore, the stripping peak current did not significantly change. According to Fig. 8, the increase in the stripping peak current decreased after 400 s of deposition. Consequently, the optimal deposition time was 400 s.

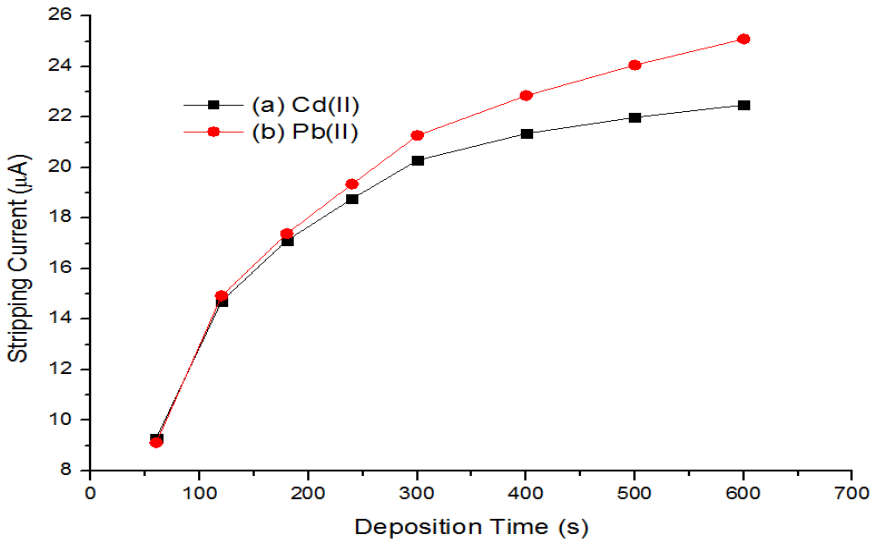

Figure 8. Relationship between the deposition time and the Cd(II) and Pb(II) stripping currents. Cd(II) and Pb(II) concentrations: 20 μg·L^{-1}. pH: 3.5. Deposition potential: -1.0 V. Bi(III) concentration: 500 μg·L^{-1}. Sb(III) concentration: 500 μg·L^{-1}.

Fig. 9 shows the effect of the Bi(III) concentration (0-1000 μg·L^{-1}) on the Cd(II) and Pb(II) stripping reactions. The largest peak current occurred at a Bi(III) concentration of 1000 μg L^{-1}, and this can be ascribed to the formation of the Sb, Cd and Pb alloy in solution, which accelerates the cation exchange process [26]. However, with a further increase in the Bi(III) concentration, the saturation amount formed by the alloy gradually decreased, and the amplitude of the stripping current also gradually decreased. Therefore, the optimal Bi(III) concentration was 700 μg L^{-1}.

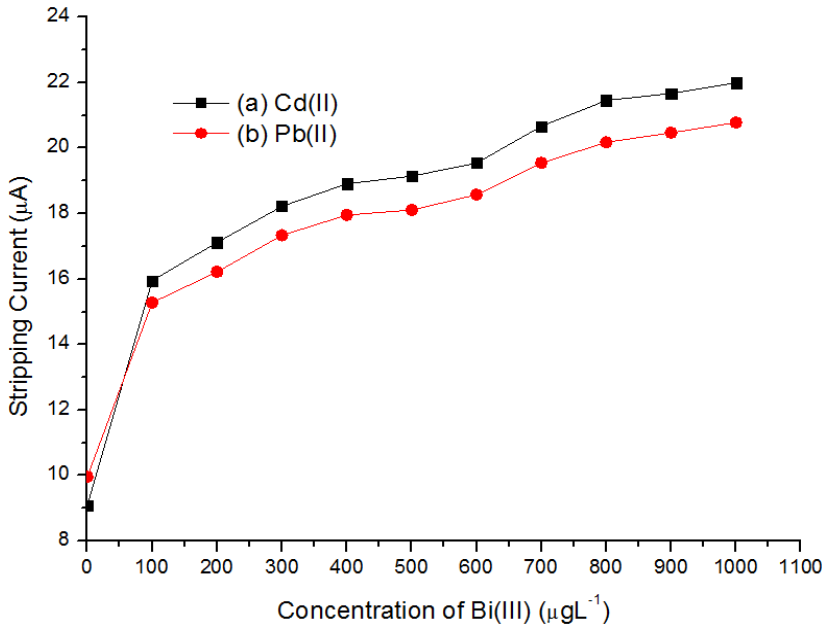

Figure 9. Relationship between the Bi(III) concentration and the Cd(II) and Pb(II) stripping currents. Cd(II) and Pb(II) concentrations: 20 μg·L^{-1}. Deposition time: 400 s. pH: 3.5. Deposition potential: -1.0 V. Sb(III) concentration: 0.

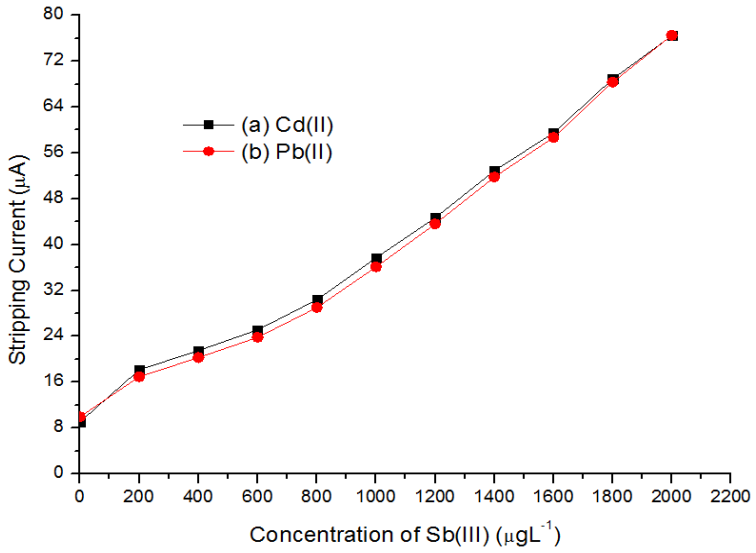

Figure 10. Relationship between the Sb(III) concentration and the Cd(II) and Pb(II) stripping currents. Cd(II) and Pb(II) concentrations: 20 μg·L^{-1}. Deposition time: 400 s. pH: 3.5. Deposition potential: -1.0 V. Bi(III) concentration: 0.

Fig. 10 shows the effect of the Sb(III) concentration (0-2000 $\mu g \cdot L^{-1}$) on the Cd(II) and Pb(II) stripping reactions. The largest peak current occurred at an Sb(III) concentration of 2000 $\mu g \cdot L^{-1}$, and this can be attributed to the formation of the Sb, Cd and Pb alloy in solution, which accelerates the cation exchange process [27]. Meanwhile, as the Sb(III) concentration increased, the alloy amount that formed gradually increased. Therefore, the optimal Sb(III) concentration was 2000 $\mu g \cdot L^{-1}$.

Fig. 11 shows the effect of the Bi(III) concentration ratio (10%-90%) in the coating buffer solution, which contains Bi(III) and Sb(III), on the Cd(II) and Pb(II) stripping reactions. The total concentration of Bi(III) and Sb(III) was 2700 $\mu g \cdot L^{-1}$, and the largest peak current appeared at a Bi(III) concentration ratio of 60%. This result can also be ascribed to the fact that Sb and Bi are in the same group and can form alloys with Cd and Pb in the buffer solution to accelerate the cation exchange process. However, the amount of alloy formed decreased in the presence of a Bi(III) concentration that was too low or too high. Consequently, the optimal Bi(III) concentration ratio was 60%.

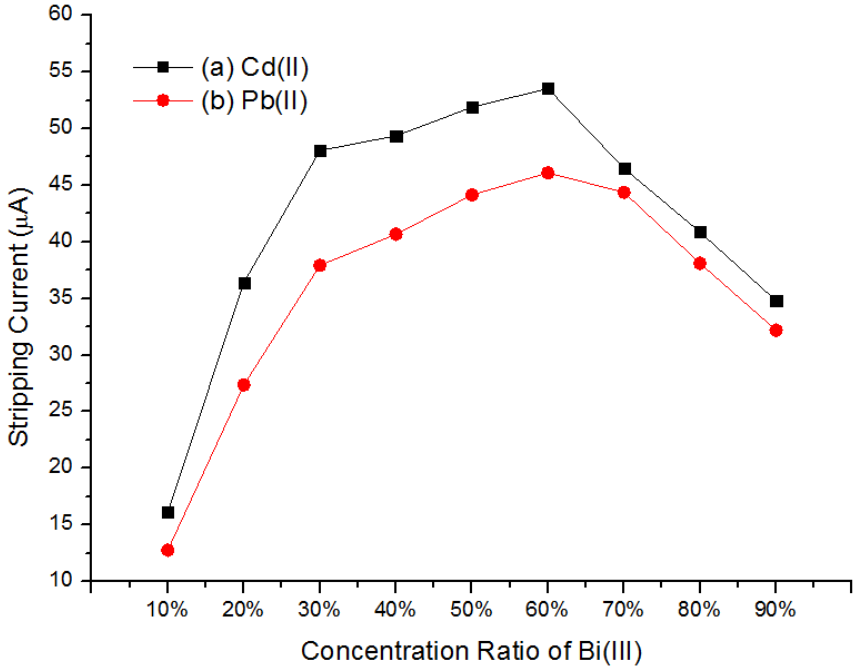

Figure 11. Relationship between the Bi(III) concentration ratio in the coating buffer solution containing Bi(III) and Sb(III) and the Cd(II) and Pb(II) stripping currents. Cd(II) and Pb(II) concentrations: 20 $\mu g \cdot L^{-1}$. Deposition time: 400 s. pH: 3.5. Deposition potential: -1.0 V. Total Bi(III) and Sb(III) concentration: 2700 $\mu g \cdot L^{-1}$.

The Cd(II) and Pb(II) stripping currents in the coating buffer solution containing Bi(III) and Sb(III) were larger than those in the coating buffer solution containing the same concentration of only Bi(III). The largest Cd(II) and Pb(II) reverse extraction currents were observed in the coating buffer solution containing only Sb(III) at a concentration of 2000 $\mu g \cdot L^{-1}$. Based on these observations, 2000 $\mu g \cdot L^{-1}$ Sb(III) was added into the buffer solution to modify the electrode using MCM41 and Nafion according to the coating method.

3.4. Analytical Performance of MCM41/Nafion/Sb/GCE

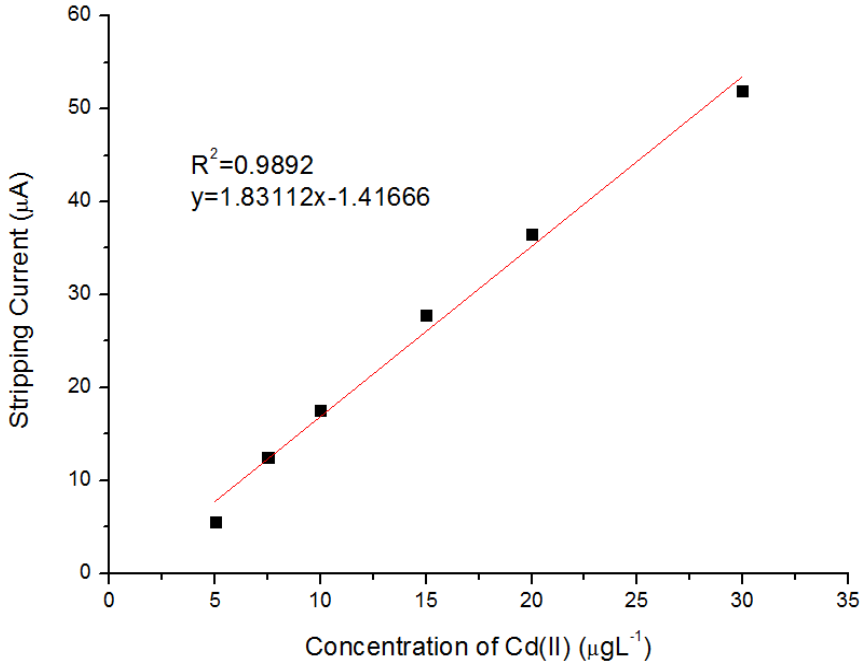

Figure 12. Corresponding calibration plots of MCM41/Nafion/Sb/GCE for different Cd(II) concentrations in a 0.1 M acetate buffer solution. pH: 3.5. Cd(II) concentration range: 5.0-30.0 μg·L^{-1}. Deposition time: 400 s. Deposition potential: -1.0 V. Sb(III) concentration: 2000 μg·L^{-1}.

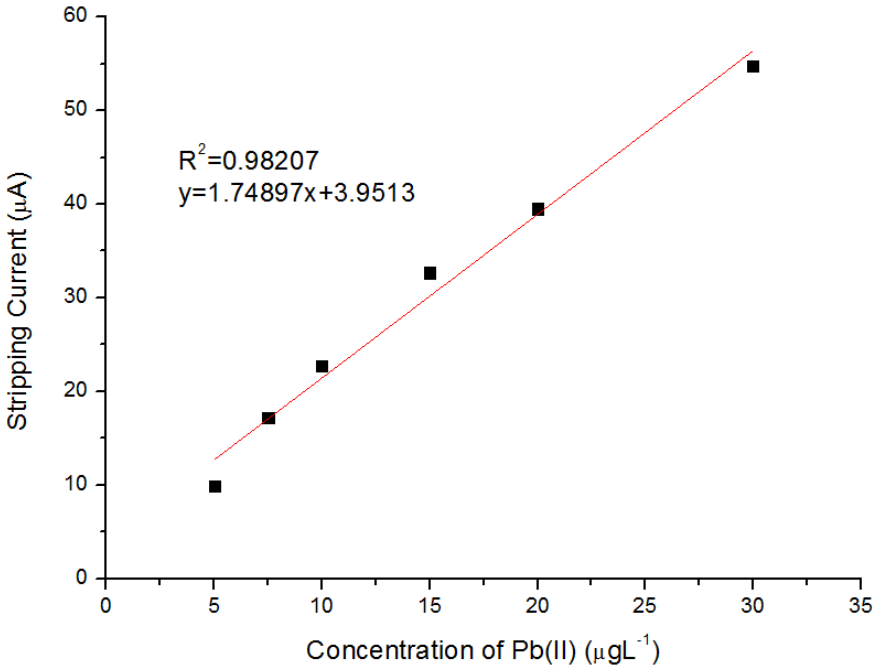

Figure 13. Corresponding calibration plots of MCM41/Nafion/Sb/GCE for different Pb(II) concentrations in a 0.1 M acetate buffer solution. pH: 3.5. Pb(II) concentration range: 5.0-30.0 μg·L^{-1}. Deposition time: 400 s. Deposition potential: -1.0 V. Sb(III) concentration: 2000 μg·L^{-1}.

The electrode prepared under the optimal conditions was used to determine the Cd(II) and Pb(II) stripping peak currents. The stripping responses at different Cd(II) and Pb(II) concentrations are

shown in Fig. 12 and Fig. 13, respectively. The peak current showed a positive linear correlation with the Cd(II) and Pb(II) concentrations (5.0-30.0 $\mu g \cdot L^{-1}$). As shown in Fig. 12, the equation y = 1.83112x-1.41666 (y: μA, x: $\mu g \cdot L^{-1}$) with a correlation coefficient of 0.9892 (S/N = 3) was obtained based on the Cd(II) calibration curve. The limit of detection (LOD) was 0.29 $\mu g \cdot L^{-1}$, and the accumulation time was 400 s. Based on Fig. 13, the equation y = 1.74897 x + 3.9513 (y: μA, x: $\mu g \cdot L^{-1}$) with a correlation coefficient of 0.98207 (S/N = 3) was obtained based on the Pb(II) calibration curve. The LOD was 0.08 $\mu g \cdot L^{-1}$, and the accumulation time was 400 s.

Table 1. Comparison of different electrodes for Cd(II) and Pb(II) determination.

Electrode	Technique	Linear range ($\mu g \cdot L^{-1}$)		LOD ($\mu g \cdot L^{-1}$)		Reference
		Cd(II)	Pb(II)	Cd(II)	Pb(II)	
CB-15-crown-5/GCE	DPASV	15.7-191.1	10.9-186.5	4.7	3.3	[28]
BioCl/MWCNT/GCE	SWASV	5-50	5-50	1.2	0.57	[29]
L-cys/GR-CS/GCE	DPASV	0.56-67.2	1.04-62.1	0.45	0.12	[5]
Bi/CNT/SPE	SWASV	2-100	2-100	0.8	0.2	[30]
Bi/C/CPE	SWASV	1-100	1-100	0.81	0.65	[31]
DMSO/GCE	ASV	50-250	5-200	3.2	1.9	[32]
MCM41/Nafion/Sb/GCE	SWASV	5-30	5-30	0.29	0.08	This work

The relative standard deviation (RSD) of 5 measurements with the same electrode was 1.73%, and the RSD for 5 electrodes prepared using the same procedure was 3.64%. The SWASV responses of the electrode to 20 $\mu g \cdot L^{-1}$ Cd(II) and Pb(II) were detected intermittently to determine the long-term stability of the electrode. Approximately 5.13% of the original response was lost after 1 week of storage under environmental conditions. The acceptable stability of the sensor can be attributed to the durability of the MCM41/Nafion composite material. Table 1 summarizes the performances of MCM41/Nafion/Sb/GCE and other reported sensors and shows the low LOD and high sensitivity of the prepared electrode.

3.5. Interference Study

Various interfering ions were added into a standard solution containing Cd(II), Pb(II) and 2000 $\mu g \cdot L^{-1}$ Sb(II) (The largest mass ratio was 100 fold.) to examine interferences. The tolerance ratio of ±5% for the Cd(II) and Pb(II) signals was satisfied in the presence of NO_3^-, SO_4^{2-}, Cl^-, K^+, Na^+, Ca^{2+}, Ag^+, Mg^{2+}, Mn^{2+}, Zn^{2+} and Al^{3+} as well as over 30-fold excess Fe^{3+}. However, once a 2-fold excess of cupric ions was added, the Cd(II) and Pb(II) stripping reactions decreased. This inhibitory effect might be related to the formation of intermetallic compounds (IMCs) and the competition between electrode surface active sites. Nevertheless, the addition of ferrocyanide ions into a test solution to form stable

and insoluble ferricyanide copper complexes could conveniently and effectively eliminate these interferences.

3.6. Soil Sample Analysis

Table 2. Cd(II) and Pb(II) recoveries in extracted soil samples.

Ion	Added ($\mu g \cdot L^{-1}$)	Found ($\mu g \cdot L^{-1}$)[a]	RSD (%)	Recovery (%)
Cd(II)	—	7.23	3.0	—
	5.0	12.12	3.6	99.1
	10.0	17.13	3.8	99.4
	20.0	26.66	4.1	97.9
Pb(II)	—	14.35	2.6	—
	5.0	18.92	3.1	97.8
	10.0	24.21	3.7	99.5
	20.0	33.52	4.2	97.6

[a]Mean of five repeat measurements

The feasibility of detecting Cd and Pb in practical samples by MCM41/Nafion/Sb/GCE was verified by analyzing extracted soil samples. The initial Cd(II) and Pb(II) concentrations were 7.23±0.04 $\mu g \cdot L^{-1}$ and 14.35±0.07 $\mu g \cdot L^{-1}$ (n = 5), respectively. The preliminary results were independently analyzed and confirmed through atomic absorption spectrometry (AAS), among which, the Cd(II) and Pb(II) concentrations were 7.45±0.03 $\mu g \cdot L^{-1}$ and 13.98±0.06 $\mu g \cdot L^{-1}$ (n = 5), respectively. The differences in the Cd(II) and Pb(II) concentrations obtained from MCM41/Nafion/Sb/GCE and AAS were lower than 5%. In addition, a recovery test was also conducted to further confirm the feasibility of using MCM41/Nafion/Sb/GCE. Table 2 shows that the average recovery rates for Cd(II) Pb(II) using the MCM41/Nafion/Sb/GCE method were 98.8% and 98.3%, respectively. These results indicate that the prepared electrode can be applied for detecting Cd(II) and Pb(II) in extracted soil samples.

4. CONCLUSION

In the present study, a novel MCM41/Nafion/Sb composite-modified GCE is introduced, and the electrode can be used to simultaneously detect Cd(II) and Pb(II). The MCM41/Nafion/Sb/GCE was studied using CV, EIS and SWASV. The large specific surface area of MCM41 resulted in superb electrochemical activity and accelerated the charge transfer dynamics of the electrode. At the same time, Nafion enhanced the stability and durability of the modified electrode. Sb formed an alloy with Cd and Pb in solution, which accelerated the cation exchange. MCM41, Nafion and Sb allow the modified electrode to be an effective, high sensitivity and low LODs sensor for detecting Cd(II) and Pb(II). The analysis of extracted soil samples further verified the feasibility of utilizing the electrode,

and satisfactory results were obtained. In addition, a green, stable, and highly sensitive electrochemical sensor was created through a composite modification of MCM41, Nafion and Sb. This sensor shows application potential for food safety and environmental monitoring.

ACKNOWLEDGEMENTS
This work was supported by the General Program of National Natural Science Foundation of China (no. 31671578) and the National High Technology Research and Development Program of China (no. 2013AA102302).

References

1. B. Bansod, T. Kumar, R. Thakur, S. Rana and I. Singh, *Biosens. Bioelectron.,* 94 (2017) 443.
2. Y. Yin, G. Zhao and G. Liu, *Int. J. Electrochem. Sci.,* 12 (2017) 5378.
3. R. Nurlzzah, L.C.K. Darvina, A.A.A. Shahrul, A.A.N. Fatimah, S.L. Faridah and Y. Norazah, *J. Electroanal. Chem.,* 799 (2017) 497.
4. M.A. Chamjangali, H. Kouhestani, F. Masdarolomoor and H. Daneshinejad, *Sens. Actuators, B,* 216 (2015) 384.
5. W. Zhou, C. Li, C. Sun and X. Yang, *Food Chem.,* 192 (2016) 351.
6. A.M. Omahony and J. Wang, *Electroanalysis,* 25 (2013) 1341.
7. M. Martin, H. Charlton, S. Bongiwe, I. Emmanuel and S. Vernon, *J. Environ. J. Environ. Sci. Health, Part A: Toxic/Hazard. Subst. Environ. Eng.,* 51 (2016) 597.
8. B. Silwana, C. Horst, E. Iwuoha and V. Somerset, *Electroanalysis,* 28 (2016) 1597.
9. D.J. Rao, J. Zhang and J.B. Zheng, *J. Iran. Chem. Soc.,* 13 (2016) 1.
10. S. Chaiyo, E. Mehmeti, K. Žagar, W. Siangproh, O. Chailapakul and K. Kalcher, *Anal. Chim. Acta,* 918 (2016) 26.
11. T. Priya, N. Dhanalakshmi and N. Thinakaran, *Int. J. Biol. Macromol.,* 104 (2017) 672.
12. Y.Y. Lu, X.Q. Liang, C. Niyungeko, J.J. Zhou and G.M. Tian, *Talanta,* 178 (2017) 324.
13. A. Benvidi, M. Nikmanesh, M.D. Tezerjani, S. Jahanbani, M. Abdollahi, A. Akbari and A. Rezaeipooranari, *J. Electroanal. Chem.,* 787 (2017) 145.
14. N. Alarcos, F. Sánchez and A. Douhal, *Microporous Mesoporous Mater.,* 683 (2017) 145.
15. B. Hilczer, E. Markiewicz, M. Polomska, J. Tritt-Goc, J. Kaszyńska, K. Pogorzelec-glaser and A. Pietraszko, *Ferroelectrics,* 472 (2014) 64.
16. F. Wang, J. Yang and K. Wu, *Anal. Chim. Acta,* 638 (2009) 23.
17. G. Zhao, Y. Yin, H. Wang, G. Liu and Z.Q. Wang, *Electrochim. Acta,* 220 (2016) 267.
18. L.Q. Xie, Y.H. Zhang, F. Gao, Q.A. Wu, P.Y. Xu, S.S. Wang, N.N. Gao and Q.X. Wang, *Chin. Chem. Lett.,* 28 (2017) 41.
19. E. Er, H. Çelikkan and N. Erk, *Sens. Actuators, B,* 238 (2017) 779.
20. K. Suzuki, R. Owen, J. Mok, H. Mochihara, T. Hosokawa, H. Kubota, H. Sakamoto and A. Matsuda, *J. Biosci. Bioeng.,* 122 (2016) 322.
21. F.A. Harraz, A.A. Ismail, S.A. Al-sayari, A. Al-hajry and M.S. Al-assiri, *Superlattices Microstruct.,* 100 (2016) 1064.
22. W.J. Yi, Y. Li, G. Ran, H.Q. Luo and N.B. Li, *Sens. Actuators, B,* 166 (2012) 544.
23. S.T. Palisoc, M.T. Natividad, N.M.D. Martinez, R.M.A. Ramos and K.A.Y. Kaw, *e-Polym,* 16 (2016) 117.
24. A.M. Ashrafi and K. Vytřas. *Talanta,* 85 (2011) 2700.
25. S.B. Hocevar, I. Švancara, B. Ogorevc and K. Vytřas. *Anal. Chem.,* 79 (2007) 8639.
26. X. Xuan, J.Y. Park, *Sens. Actuators, B,* 255 (2017) 1220.
27. Z. Wang, K. Wang, L. Zhao, S.G. Chai, J.Z. Zhang, X.H. Zhang and Q.C. Zou, *Mater. Sci. Eng., C,*

80 (2017) 180.
28. N. Serrano, A.G. Calabuig and M. Valle, *Talanta,* 138 (2015) 130.
29. S. Cerovac, V. Guzsvány, Z. Kónya, A.M. Ashrafi, I. Švancara, S. Rončević, A. Kukovecz and B. Dalmacija, *Talanta,* 134 (2015) 640.
30. U. Injang, P. Noyrod, W. Siangproh, W. Dungchai, S. Motomizu and O. Chailapakul, *Anal. Chim. Acta,* 668 (2010) 54.
31. P.F. Niu, C. Fernández-sánchez, M. Gich, C. Ayora and A. Roig, *Electrochim. Acta,* 165 (2015) 155.
32. S.M. Rosolina, J.Q. Chambers, C.W. Lee and Z.L. Xue, *Anal. Chim. Acta,* 893 (2015) 25.